A Comparative Study on Overall Efficiency of Two-Dimensional Wireless Power Transfer Systems Using Rotational and Directional Methods

Hanwei Wang , Cheng Zhang , *Member, IEEE*, Yun Yang , *Member, IEEE*,
Hui Wen Rebecca Liang , *Student Member, IEEE*, and Shu Yuen Ron Hui , *Fellow, IEEE*

Abstract—Two-dimensional (2-D) wireless power transfer (WPT) systems can be controlled by either the directional method or the rotational method. The rotational method refers to the use of omnidirectional transmitter generating rotational flux regardless of the load positions, while the directional method refers to the use of omnidirectional transmitter generating magnetic flux directly toward the power-consuming load directions. This article compares the overall efficiency of the two methods for 2-D WPT systems. Theoretical analysis reveals that the directional WPT can be more efficient than the rotational WPT with either single or multiple loads when the magnetic field vector is controlled within the feasible zones; and the efficiency difference between the two methods are more significant when the dimensions of the receiver coils are smaller. Both simulation and experimental results are consistent in validating the two discoveries. They indicate that the averaged efficiency of the directional method is at least 5% higher than that of the rotational one.

Index Terms—Directional method, rotational method, two-dimensional (2-D), wireless power transfer (WPT).

Hanwei Wang is with the Department of Electrical and Computer Engineering, University of Illinois Urbana-Champaign, Champaign, IL 61820 USA (e-mail: hanweiw2@illinois.edu).

Cheng Zhang is with the Department of Electrical and Electronic Engineering, University of Manchester, Manchester M13 9PL, U.K. (e-mail: cheng.zhang@manchester.ac.uk).

Yun Yang is with the Department of Electrical Engineering, Hong Kong Polytechnic University, Hong Kong (e-mail: yun1989.yang@polyu.edu.hk).

Hui Wen Rebecca Liang is with the Department of Electrical and Electronic Engineering, University of Hong Kong, Hong Kong (e-mail: rebeccaliang0425@gmail.com).

Shu Yuen Ron Hui was with the University of Hong Kong, Hong Kong. He is now with the School of Electrical and Electronic Engineering, Nanyang Technological University, Singapore 639798, and also with the Department of Electrical and Electronic Engineering, Imperial College London, South Kensington SW7 2BU, U.K. (e-mail: ron.hui@ntu.edu.sg).

Color versions of one or more figures in this article are available at https://doi.org/10.1109/TIE.2020.3048317.

Digital Object Identifier 10.1109/TIE.2020.3048317

I. INTRODUCTION

RECENT advancements have enabled wireless power transfer (WPT) to reach wide-spread commercialization stage with the success of the Qi standard launched in 2010 by the wireless power consortium (WPC), now comprising over 550 companies worldwide [1]. Wireless charging pads for portable electronics such as mobile phones are not only available for domestic and office applications, they are also widely installed inside many new vehicles for charging mobile phones and other Qi-compatible devices. So far, most of the WPT applications based on near-field magnetic resonance [2] are of directional nature, meaning that the wireless power transmitters are designed to transmit wireless power directionally toward an area where the load with the receiver coil will be placed [3]–[6].

Omni-directional WPT systems have been reported in [7]–[16]. Among them, [7] has addressed an omnidirectional WPT system comprising a transmitter with three orthogonal coils and a receiver also with three orthogonal coils (Fig. 1). In [7], several methods covering periodic switching of the plane of rotation, frequency shift, single-axis amplitude modulation, double-axis amplitude modulation, and wide-band operation have been discussed for omnidirectional magnetic field generation. Based on the same orthogonal coils, [8] demonstrates that receiver coil can obtain wireless power at positions of multiple angles around the orthogonal transmitter structure. Reference [9] adopts three orthogonal-coil structures for both the transmitter and receiver module. However, an important principle has been pointed out in [10] and [11] that identical currents used in the orthogonal transmitter coils in [7]–[9] cannot generate magnetic flux vector in a true omnidirectional manner. Nonidentical current control has to be used for true omnidirectional WPT systems [10], [11]. Nonidentical current control has been further elaborated and generalized into a set of general control principle for detecting load positions and directing wireless power towards the loads in [12]. The general mathematical analyses of 2-D and 3-D WPT systems can be found in [13] and [14], respectively. A modified three-transmitter-coil structure in the bowl or wok shape is reported in [15]. In order to develop load independent resonance for variable coupling situation in omnidirectional WPT systems, high-order resonant circuits are explored in [16]. High degree
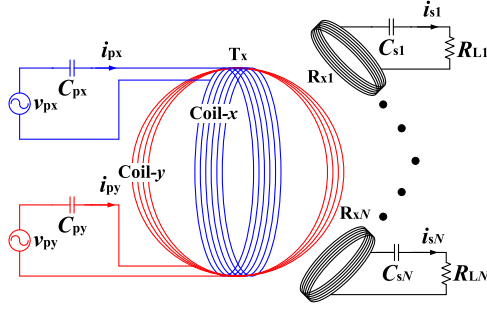
Fig. 1. Circuit diagram of a 2-D WPT system with multiple loads.

of spatial freedom for WPT can also be achieved with the use of large dipole structures [17]. In [18], receiver resonators are tuned at different frequencies so that the omnidirectional transmitter structure can select the load according to their respective tuned frequencies.

So far, limited literature has investigated the overall efficiency of omnidirectional WPT systems with the general control methods, i.e., the rotational method and the directional method. The rotational method is implemented by the phase angle modulation of transmitter currents and the generating magnetic field vector can rotate in a circle regardless of load positions [11]. The directional method is achieved by the amplitude modulation of transmitter currents and the generating magnetic field vector can point toward one direction according the positions of power consuming loads [12]. This article bridges the research gap by comparing the overall efficiency of a 2-D WPT system with the two control methods. Practical results justify that the directional method can be more efficient than the rotational method when the magnetic field vector is controlled within the feasible zones, particularly when the receiver coil sizes become smaller.

II. EFFICIENCY ANALYSIS OF 2-D WPT SYSTEMS

A. General Analysis of the System

A typical 2-D WPT system with multiple loads is depicted in Fig. 1. The transmitter (Tx) consists of two orthogonal coils, i.e., an x-axis coil (Coil-x) and a y-axis coil (Coil-y). The N numbers of receivers (Rx) are distributed around the Tx to pick up energy. Both the Tx and Rx are in series compensation to minimize the apparent power rating of the power supply and maximize the transfer capability, respectively,

$$\omega_{\mathrm{o}}^2 = \frac{1}{L_{\mathrm{px}}C_{\mathrm{px}}} = \frac{1}{L_{\mathrm{py}}C_{\mathrm{py}}} = \frac{1}{L_{sn}C_{sn}} \quad (n = 12, \ldots, N)$$
(1)

where L_{px}, L_{py}, and L_{sn} are the inductances of the Tx and Rx; C_{px}, C_{py}, and C_{sn} are the compensated capacitances; ω_{o} is the resonant angular frequency.

Based on the circuit diagram, the M-model of the circuitry in the frequency-domain can be given as follows:

$$\begin{bmatrix} \mathbf{V_P} \\ \mathbf{O} \end{bmatrix} = \begin{bmatrix} \mathbf{Z_P} & -j\omega\mathbf{M_{TR}^T} \\ -j\omega\mathbf{M_{TR}} & \mathbf{Z_s} \end{bmatrix} \begin{bmatrix} \mathbf{I_P} \\ \mathbf{I_s} \end{bmatrix}$$
(2)

where

$$\mathbf{V_P} = \begin{bmatrix} v_{\mathrm{px}} \\ v_{\mathrm{py}} \end{bmatrix}, \mathbf{I_P} = \begin{bmatrix} i_{\mathrm{px}} \\ i_{\mathrm{py}} \end{bmatrix}, \mathbf{I_s} = \begin{bmatrix} i_{s1} \\ i_{s2} \\ \vdots \\ i_{sN} \end{bmatrix},$$

$$\mathbf{Z_P} = \begin{bmatrix} Z_{\mathrm{px}} & 0 \\ 0 & Z_{\mathrm{py}} \end{bmatrix}, \mathbf{M_{TR}} = \begin{bmatrix} M_{\mathrm{xR1}} & M_{\mathrm{yR1}} \\ M_{\mathrm{xR2}} & M_{\mathrm{yR2}} \\ \vdots & \vdots \\ M_{\mathrm{xRN}} & M_{\mathrm{yRN}} \end{bmatrix}$$

$$\mathbf{Z_s} = \begin{bmatrix} Z_{s1} & j\omega M_{\mathrm{R1R2}} & \cdots & j\omega M_{\mathrm{R1RN}} \\ j\omega M_{\mathrm{R1R2}} & Z_{s2} & \cdots & j\omega M_{\mathrm{R2RN}} \\ \vdots & \vdots & \ddots & \vdots \\ j\omega M_{\mathrm{R1RN}} & j\omega M_{\mathrm{R2RN}} & \cdots & Z_{sN} \end{bmatrix}$$

$Z_{\mathrm{px}} = j\omega L_{\mathrm{px}} + \frac{1}{j\omega C_{\mathrm{px}}} + r_{\mathrm{px}}$, $Z_{\mathrm{py}} = j\omega L_{\mathrm{py}} + \frac{1}{j\omega C_{\mathrm{py}}} + r_{\mathrm{py}}$, $Z_{sn} = j\omega L_{sn} + \frac{1}{j\omega C_{sn}} + r_{sn} + R_{\mathrm{L}n}$ $(n = 12, \ldots, N)$; v_{px}, v_{py}, i_{px}, and i_{py} are the input voltages and currents of Tx; i_{sn} are the currents of Rx; r_{px}, r_{py}, and r_{sn} are the equivalent series resistances (ESR) of Tx and Rx; $R_{\mathrm{L}n}$ are the load resistances; $M_{\mathrm{xR}n}$ and $M_{\mathrm{yR}n}$ are the mutual inductances between Tx and Rx; $M_{\mathrm{R}n\mathrm{R}m}$ $(m = 12, \ldots, N, m \neq n)$ are the mutual inductances between Rx; ω is the operating angular frequency. Generally, the mutual inductances between Rx are negligible, i.e., $M_{\mathrm{R}n\mathrm{R}m} = 0$ and the switching frequency is operated at the resonant frequency, i.e., $\omega = \omega_{\mathrm{o}}$. Based on (2), the currents of Rx can be derived as follows:

$$i_{sn} = \frac{j\omega_{\mathrm{o}}M_{\mathrm{xR}n}i_{\mathrm{px}} + j\omega_{\mathrm{o}}M_{\mathrm{yR}n}i_{\mathrm{py}}}{j\omega_{\mathrm{o}}L_{sn} + \frac{1}{j\omega_{\mathrm{o}}C_{sn}} + r_{sn} + R_{\mathrm{L}n}} \quad (n = 12, \ldots, N)$$
(3.1)

By substituting (1) into (3.1),

$$i_{sn} = \frac{j\omega_{\mathrm{o}}M_{\mathrm{xR}n}i_{\mathrm{px}} + j\omega_{\mathrm{o}}M_{\mathrm{yR}n}i_{\mathrm{py}}}{r_{sn} + R_{\mathrm{L}n}} \quad (n = 12, \ldots, N)$$
(3.2)

The total efficiency the 2-D WPT system is

$$\eta = \frac{\sum_{n=1}^{N} R_{\mathrm{L}n}|i_{sn}|^2}{\sum_{n=1}^{N} R_{\mathrm{L}n}|i_{sn}|^2 + r_{\mathrm{px}}|i_{\mathrm{px}}|^2 + r_{\mathrm{py}}|i_{\mathrm{py}}|^2}$$
(4)

By substituting (3.2) into (4),

$$\eta =$$

$$\frac{\sum_{n=1}^{N} K_{1n}|i_{\mathrm{px}}|^2 + K_{2n}|i_{\mathrm{py}}|^2 + K_{3n}i_{\mathrm{px}} \cdot i_{\mathrm{py}}}{\sum_{n=1}^{N} (K_{1n} + r_{\mathrm{px}})|i_{\mathrm{px}}|^2 + (K_{2n} + r_{\mathrm{py}})|i_{\mathrm{py}}|^2 + K_{3n}i_{\mathrm{px}} \cdot i_{\mathrm{py}}}$$
(5)

where $K_{1n} = \frac{\omega_{\mathrm{o}}^2 M_{\mathrm{xR}n}^2 R_{\mathrm{L}n}}{(r_{sn}+R_{\mathrm{L}n})^2}$, $K_{2n} = \frac{\omega_{\mathrm{o}}^2 M_{\mathrm{yR}n}^2 R_{\mathrm{L}n}}{(r_{sn}+R_{\mathrm{L}n})^2}$, and $K_{3n} = \frac{2\omega_{\mathrm{o}}^2 M_{\mathrm{xR}n} M_{\mathrm{yR}n} R_{\mathrm{L}n}}{(r_{sn}+R_{\mathrm{L}n})^2}$.

B. Efficiency of the System Using the Rotational Method

The resultant magnetic field vector of the 2-D WPT system can rotate in a circular manner (as shown in Fig. 2) by controlling the currents of Tx with the same magnitude I_{m} but 90° phase
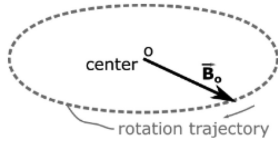
Fig. 2. Typical magnetic field vector of the 2-D WPT system using the rotational method.
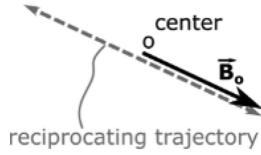

Fig. 3. Typical magnetic field vector of the 2-D WPT system using the directional method.

shift, i.e.,

$$\begin{cases} i_{\mathrm{px}} = I_m e^{j\omega t} \\ i_{\mathrm{py}} = I_m e^{j\left(\omega t + \frac{\pi}{2}\right)} \end{cases}. \tag{6}$$

This control method is called "rotational" method. The ability of rotating the magnetic field vector in a circular manner is equivalent to that of omnidirectional magnetic field vector in a 2-D sense. A receiving coil placed anywhere near the transmitter structure is able to pick-up a certain level of oscillating magnetic field.

By substituting (6) into (5), the overall efficiency of the 2-D WPT system controlled by the rotational method can be derived as follows:

$$\eta_{\mathrm{rot}} = \frac{\sum_{n=1}^{N} K_{1n} + K_{2n}}{\sum_{n=1}^{N} K_{1n} + K_{2n} + r_{\mathrm{px}} + r_{\mathrm{py}}}. \tag{7}$$

C. Efficiency of the System Using the Directional Method

The trajectory of the magnetic field vector of the 2-D WPT system can also form a straight line (as shown in Fig. 3) by controlling the currents of Tx in phase but different magnitudes, i.e.,

$$\begin{cases} i_{\mathrm{px}} = I_m \cos\theta e^{j\omega t} \\ i_{\mathrm{py}} = I_m \sin\theta e^{j\omega t} \end{cases} \tag{8}$$

where $\cos\theta$ and $\sin\theta$ are the amplitude modulation functions of i_{px} and i_{py}.

This control method is called "directional" method. By regulating the physical angle of the resultant magnetic field vector θ ($0°\leq\theta<360°$), the current amplitudes of Tx can be theoretically controlled to reach any points in the space near the 2-D transmitting coil. When a single receiver coil is placed, the maximum efficiency of the WPT system can be achieved by controlling the central magnetic field to vertically penetrate the receiver coil plane.

By substituting (8) into (5), the overall efficiency of the 2-D WPT system controlled by the directional method can be derived

as follows:

$$\eta_{\mathrm{dir}} =$$

$$\frac{\sum_{n=1}^{N} K_{1n}\cos^2\theta + K_{2n}\sin^2\theta + K_{3n}\sin\theta\cos\theta}{\sum_{n=1}^{N}\left(K_{1n}+r_{\mathrm{px}}\right)\cos^2\theta+\left(K_{2n}+r_{\mathrm{py}}\right)\sin^2\theta+K_{3n}\sin\theta\cos\theta}. \tag{9}$$

D. Comparisons of the Two Methods

The efficiency difference between the two methods can be derived by subtracting (9) to (7), as given in (10.1) shown at the bottom of the next page, where

$$\Delta H = K_{4n}\sin2\theta + K_{5n}\cos2\theta \tag{10.2}$$

$$K_{4n} = \sum_{n=1}^{N} \frac{\omega_o^2 R_{\mathrm{L}n}}{\left(r_{\mathrm{s}n} + R_{\mathrm{L}n}\right)^2} M_{\mathrm{xR}n} M_{\mathrm{yR}n}\left(r_{\mathrm{px}} + r_{\mathrm{py}}\right) \tag{10.3}$$

$$K_{5n} = \sum_{n=1}^{N} \frac{\omega_o^2 R_{\mathrm{L}n}}{\left(r_{\mathrm{s}n} + R_{\mathrm{L}n}\right)^2}\left(r_{\mathrm{py}}M_{\mathrm{xR}n}^2 - r_{\mathrm{px}}M_{\mathrm{yR}n}^2\right) \tag{10.4}$$

In (10.2), if $K_{4\mathrm{n}} > 0$,

$$\Delta H = \sqrt{K_{4n}^2 + K_{5n}^2}\,\sin\left(2\theta + \tan^{-1}\frac{K_{5n}}{K_{4n}}\right) \tag{10.5}$$

If $K_{4\mathrm{n}} < 0$,

$$\Delta H = \sqrt{K_{4n}^2 + K_{5n}^2}\,\sin\left(2\theta + \tan^{-1}\frac{K_{5n}}{K_{4n}} + \pi\right) \tag{10.6}$$

where $-\frac{\pi}{2} < \tan^{-1}\frac{K_{5n}}{K_{4n}} < \frac{\pi}{2}$.

If $K_{4n} = 0$,

$$\Delta H = K_{5n}\cos2\theta. \tag{10.7}$$

Based on (10.5), (10.6), and (10.7), the schematic diagram of the efficiency difference between the two methods can be depicted from the topic-view of the Tx, as shown in Fig. 4. When the magnetic field vector of the directional method is controlled in the feasible zones, the overall efficiency of the 2-D WPT system controlled by the directional method is higher than the rotational method.

For single Rx located in the typical eight positions of 2-D WPT systems, as presented in Fig. 5, the efficiency difference of the two methods can be further derived based on (10.1), as given in (11.1) shown at the bottom of the next two pages. Here, to simplify the analysis without loss of generality, the ESR of coil-x and coil-y is assumed to be equal (i.e., $r_{\mathrm{px}} = r_{\mathrm{py}} = r_p$) and the mutual inductances of the eight cases are listed in Table I. Based on (11.1), the maximum and minimum efficiency differences (i.e., $\Delta\eta_{\mathrm{max}}$ and $\Delta\eta_{\mathrm{min}}$ in (11.2) and (11.3), respectively) can be derived by solving $\frac{\partial\Delta\eta}{\partial\theta} = 0$. For all the eight cases,

$$\Delta\eta_{\mathrm{max}} = \frac{\frac{\omega_o^2 M^2}{(r_{\mathrm{s}1}+R_{\mathrm{L}1})^2}R_{\mathrm{L}1}r_p}{\left[\frac{\omega_o^2 M^2}{(r_{\mathrm{s}1}+R_{\mathrm{L}1})^2}R_{\mathrm{L}1} + r_p\right]\left[\frac{\omega_o^2 M^2}{(r_{\mathrm{s}1}+R_{\mathrm{L}1})^2}R_{\mathrm{L}1} + 2r_p\right]} \tag{11.2}$$
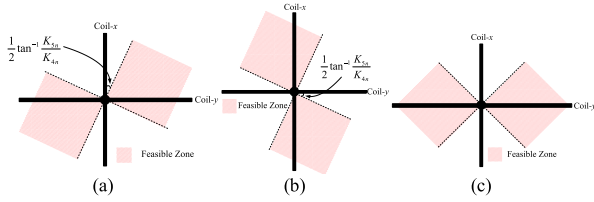
$$\Delta\eta_{\mathrm{min}} = 0 \tag{11.3}$$

Fig. 4. Schematic diagram of the efficiency difference between the two methods. (a) $K_{4n} > 0$. (b) $K_{4n} < 0$. (c) $K_{4n} = 0$.

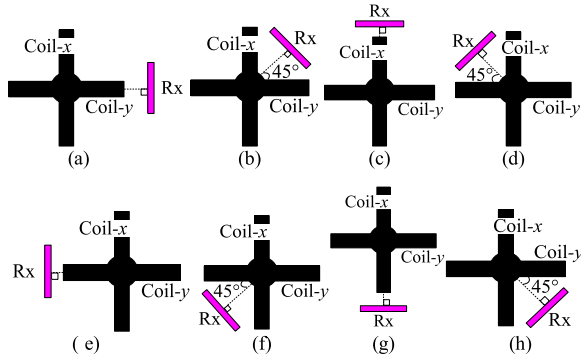Fig. 5. Typical eight positions of single Rx in the 2-D WPT system.

TABLE I
PARAMETERS OF THE EIGHT-POSITION CASES

Positions	(M_{xR1}, M_{yR1})	$\Delta\eta_{\max}$	$\Delta\eta_{\min}$
Fig. 5(a)	$(M, 0)$	$\theta = 0$ or $\theta = \pi$	$\theta = \frac{\pi}{2}$ or $\theta = \frac{3\pi}{2}$
Fig. 5(b)	$\left(\frac{M}{\sqrt{2}}, \frac{M}{\sqrt{2}}\right)$	$\theta = \frac{\pi}{4}$ or $\theta = \frac{5\pi}{4}$	$\theta = \frac{3\pi}{4}$ or $\theta = \frac{7\pi}{4}$
Fig. 5(c)	$(0, M)$	$\theta = \frac{\pi}{2}$ or $\theta = \frac{3\pi}{2}$	$\theta = 0$ or $\theta = \pi$
Fig. 5(d)	$\left(-\frac{M}{\sqrt{2}}, \frac{M}{\sqrt{2}}\right)$	$\theta = \frac{3\pi}{4}$ or $\theta = \frac{7\pi}{4}$	$\theta = \frac{\pi}{4}$ or $\theta = \frac{5\pi}{4}$
Fig. 5(e)	$(-M, 0)$	$\theta = 0$ or $\theta = \pi$	$\theta = \frac{\pi}{2}$ or $\theta = \frac{3\pi}{2}$
Fig. 5(f)	$\left(-\frac{M}{\sqrt{2}}, -\frac{M}{\sqrt{2}}\right)$	$\theta = \frac{\pi}{4}$ or $\theta = \frac{5\pi}{4}$	$\theta = \frac{3\pi}{4}$ or $\theta = \frac{7\pi}{4}$
Fig. 5(g)	$(0, -M)$	$\theta = \frac{\pi}{2}$ or $\theta = \frac{3\pi}{2}$	$\theta = 0$ or $\theta = \pi$
Fig. 5(h)	$\left(\frac{M}{\sqrt{2}}, -\frac{M}{\sqrt{2}}\right)$	$\theta = \frac{3\pi}{4}$ or $\theta = \frac{7\pi}{4}$	$\theta = \frac{\pi}{4}$ or $\theta = \frac{5\pi}{4}$

The corresponding phase angle of the directional method for achieving $\Delta\eta_{\max}$ and $\Delta\eta_{\min}$ are provided in Table I.

Based on (11.2), the plot of M^2-$\Delta\eta_{\max}$ can be depicted, as shown in Fig. 6. Here,

$$M_{\max} = \frac{\sqrt{2}(r_{s1} + R_{L1})^2 r_p}{\omega_o^2 R_{L1}} \qquad (12)$$

TABLE II
PARAMETERS OF THE PRACTICAL SETUP

Parameter Name	Value
Transmitting coil diameter d_{Tx}	31 cm
Transmitting coil number of turns N_{Tx}	11
Transmitting coil inductance L_{Tx}	86.86 µH
Transmitting coil serial capacitance C_{Tx}	1 nF
Transmitting coil parasitic resistance R_{Tx}	1.61 Ω
Receiving coil diameter d_{Rx}	31 cm/20 cm
Receiving coil number of turns N_{Rx}	11
Receiving coil inductance L_{Rx}	86.35 µH/49.88 µH
Receiving coil serial capacitance C_{Rx}	1 nF/1.75 nF
Receiving coil parasitic resistance R_{Rx}	1.61 Ω/1.04 Ω
Load resistance R_{Load}	3.24 Ω
Power source frequency f	540 kHz

When the mutual inductance M equals to $M_{\max}$, $\Delta\eta_{\max}$ is maximized. For practical 2-D WPT systems, $M > M_{\max}$ always holds, which means a smaller M giving rise to a larger $\Delta\eta_{\max}$, and vice versa. For two Rx coils at the same position but with different sizes, due to the mutual inductance of the smaller Rx coil is smaller than that of the larger Rx coil, the advantages of gaining higher efficiency by the directional method is more prominent for the 2-D WPT system with single Rx.

III. IMPLEMENTATION AND EVALUATION

Experiments are conducted based on the practical setup, the schematic of which is shown in Fig. 7. A photograph of the hardware setup is shown in Fig. 8. Only the *x*-axis and the *y*-axis of the 3-D transmitter are adopted to deliver power for the 2-D WPT system, while the *z*-axis of the 3-D transmitter remains open circuit. The high-frequency power supplies for both the *x*- and *y*-axis coils of the transmitting coil are implemented by the Tektronics AFG3102 dual channel function generator and the AR 25A250A RF power amplifier. The amplitude and the frequency of the sinusoidal signals provided by the function generator are controlled via the interface of MATLAB in the PC. Both the *x*- and *y*-axis coils of the transmitting coil are constructed with Litz wires and have 11 turns. The diameters for both the *x*- and *y*-axis coils are 31 cm. *Rx* coils of two different diameters are used in the experiment. The large *Rx* coil has a diameter of 31 cm while the small *Rx* coil has a diameter of 20 cm. The Rx coil resonator is loaded with a resistor of 3.24 Ω. The nominal parameters of the experiment setup are tabulated in Table II.

$$\Delta\eta = \eta_{\text{dir}} - \eta_{\text{rot}} = \frac{\Delta H}{\left[\sum_{n=1}^{N} (K_{1n} + r_{\text{px}}) \cos^2\theta + (K_{2n} + r_{\text{py}}) \sin^2\theta + K_{3n} \sin\theta\cos\theta\right]\left[\sum_{n=1}^{N} K_{1n} + K_{2n} + r_{\text{px}} + r_{\text{py}}\right]} \qquad (10.1)$$
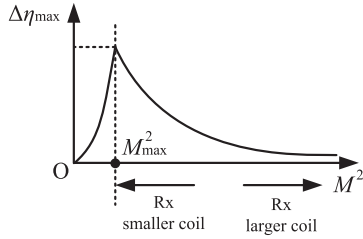
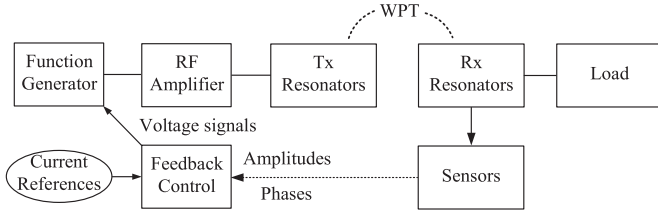Fig. 6. Plot of M²-Δηmax based on the parameters of the eight-position cases.

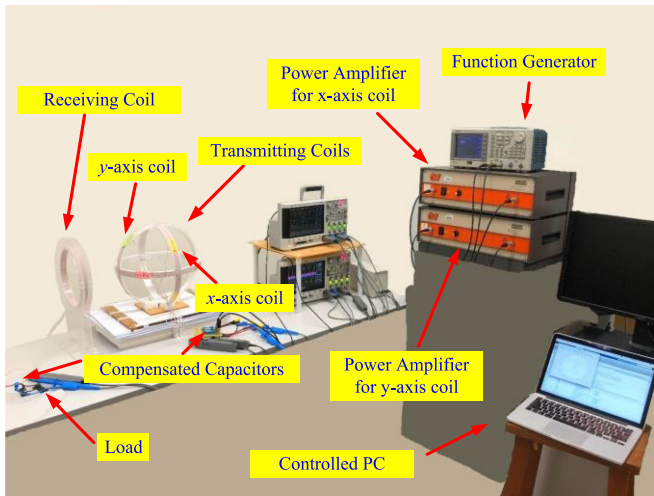Fig. 7. Schematic of the experimental setup for the 2-D WPT system.

Fig. 8. Photograph of the practical setup.

TABLE III
CASES INVESTIGATED FOR A SINGLE RECEIVER

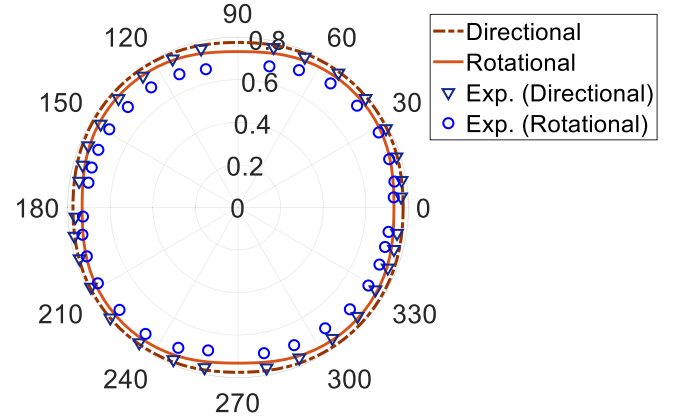| Case	Rx coil diameter (cm)	Distance between Rx and Tx (cm)
1	31	30
2	31	40
3	20	30
4	20	40

Fig. 9. Simulation and experimental efficiency curves of case 1.
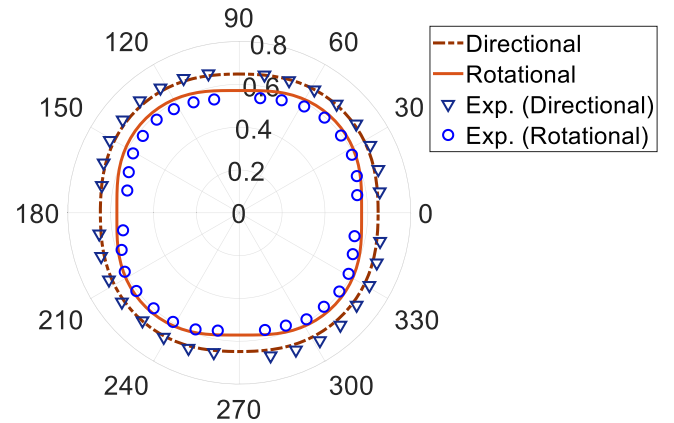
Fig. 10. Simulation and experimental efficiency curves of case 2.

A. Efficiency Comparisons of the Rotational and Directional WPT Methods for a Single Receiver

For the 2-D WPT system with a single receiver, four cases are studied, as tabulated in Table III. The large Rx coil is adopted in cases 1 and 2, whereas the small Rx coil is adopted in cases 3 and 4. The load is placed in a range of angular locations with the Rx coil plane around and facing the center of the Tx structure at two fixed distances. The distance of 30 cm is adopted in cases 1 and 3, whereas the distance of 40 cm is adopted in cases 2 and 4. At each load location, the energy efficiency is

obtained from the ratio of the load power and the input power of the transmitter. For the directional WPT tests, the two Tx coil currents will be programmed to generate a resultant magnetic field vector pointing directly toward the Rx coil center in each load location. The efficiency measurements taken with the Rx coil around the Tx structure over one cycle are expected to be the maximum efficiency point for that angular direction.

Note that the 2-D WPT system can be driven directly by power inverters. The power amplifiers are used only for convenience

$$\Delta\eta = \frac{\frac{\omega_o^2 R_{L1} r_p}{(r_{s1}+R_{L1})^2} \left[\left(M_{xR1}^2 - M_{yR1}^2 \right) \cos 2\theta + 2M_{xR1}M_{yR1} \sin 2\theta \right]}{\left[\frac{\omega_o^2 R_{L1}}{(r_{s1}+R_{L1})^2} \left(M_{xR1} \cos \theta + M_{yR1} \sin \theta \right)^2 + r_p \right] \left[\frac{\omega_o^2 R_{L1}}{(r_{s1}+R_{L1})^2} \left(M_{xR1}^2 + M_{yR1}^2 \right) + 2r_p \right]} \tag{11.1}$$
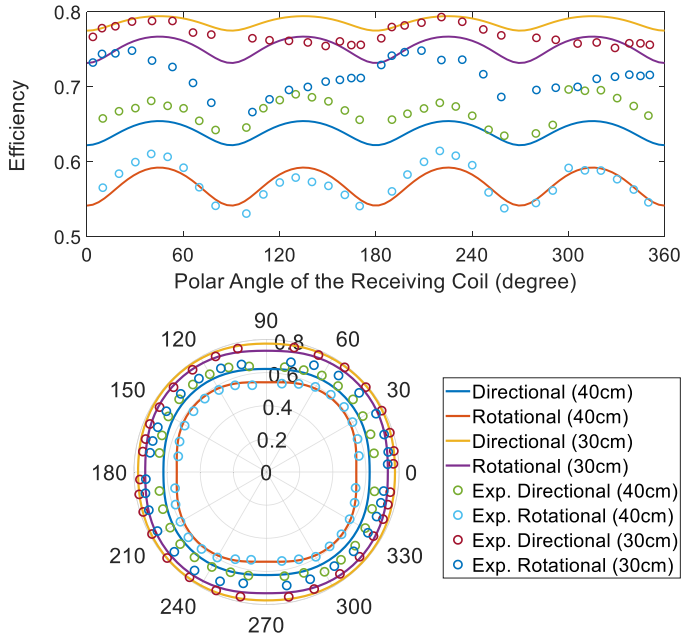
Fig. 11. Comparative results of cases 1 and 2 for the large Rx coil.

Fig. 12. Simulation and experimental efficiency curves of case 3.

Fig. 13. Simulation and experimental efficiency curves of case 4.

sake. The loss in the power source is therefore not considered in the comparison. The polar plot of the efficiency-angle curve for the case 1 is shown in Fig. 9 when the large *Rx* coil is placed at a distance of 30 cm from the center of the Tx structure. Here, the "solid" and "dashed" lines are the simulation results while the "triangle" and "circle" patterns are the practical measurements. It can be observed that the simulation results are highly consistent with the practical measurements for both methods. The directional WPT method achieves a higher efficiency than the rotational WPT method at any positions, which validates the analysis and the derived equations in (11). Therefore, it is reasonable to state that, in the case of a single load situation, the best approach is to do the scanning process, determine the load position and then zoom the wireless power toward the load directionally. This principle applies equally well even if the single load is placed further away from 30 to 40 cm as shown in Fig.10 for the case 2, although a longer transmission distance leads to a reduction in the energy efficiency. When putting the results of Figs. 9 and 10 in one polar plot, Fig. 11 shows that the theoretical results are highly consistent with the practical measurements. Efficiency of directional and rotational method of two distances plotted in Cardioid coordinate and polar coordinate. The results confirm that the analysis is sufficiently accurate.

When the large Rx coil is replaced with the small counterpart with a diameter of 20 cm, the same sets of tests are repeated and the corresponding results are shown in Figs. 12 and 13. Obviously, a *Rx* coil with a small diameter has a lower efficiency than that of a large diameter for the same *Tx* structure. The reason is that a smaller coil will pick up less output power. Again, combining the results of Figs. 12 and 13 in one polar plot (Fig. 14) shows that the analysis is reliable and accurate. The efficiency measurements of directional and rotational method
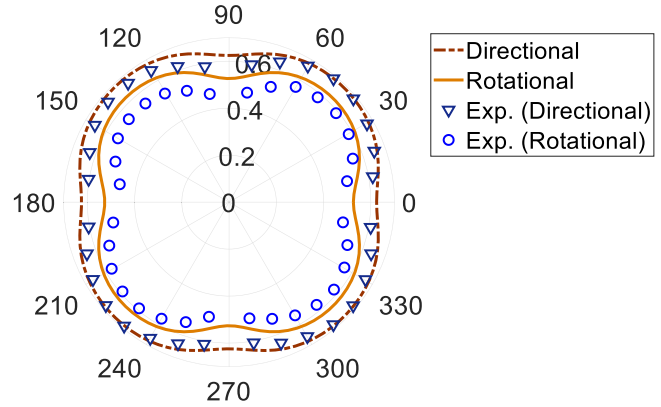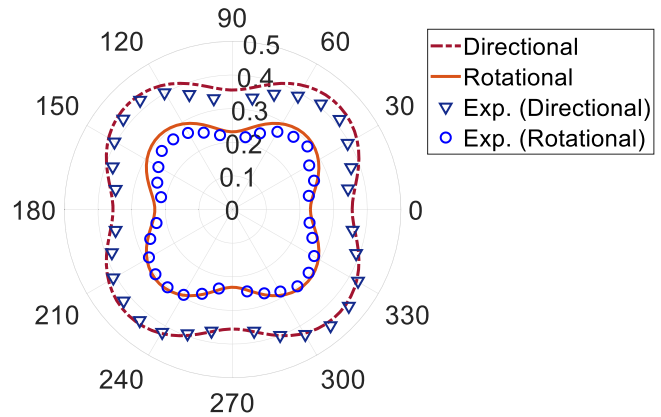
of two distances are plotted in Cardioid coordinate and polar coordinate. The efficiency differences of the two methods between the large *Rx* coil and small *Rx* coil are plotted in Fig. 15. Both simulation and experimental results confirm the analysis in Fig. 6 that the efficiency differences between the two methods are more significant for a smaller Rx coil.

B. Efficiency Comparisons of the Rotational and Directional WPT Methods for Multiple Receivers

For the 2-D WPT system with multiple receivers, 12 cases of WPT systems with two Rx coils (i.e., Rx-1 and Rx-2) are examined, as tabulated in Table IV. Both the parameters of small and large Rx coils are the same as the parameters given in Table II, while the load conditions are different. "Load-1" indicates the load connected to the Rx-1 and "Load-2" indicates the load connected to the Rx-1 "open" means no load is connected. The Rx coils are placed in two different sets of positions, as shown in Fig 16. The distance between the Tx and the Rx-1 or Rx-2 are fixed at 30 cm.

For the rotational method, due to the two receivers are placed in fixed positions, the overall efficiency of the loads almost remains constant for each case. The overall efficiencies of the rotational WPT for the 12 cases in both simulation and experiment are provided in Table V.
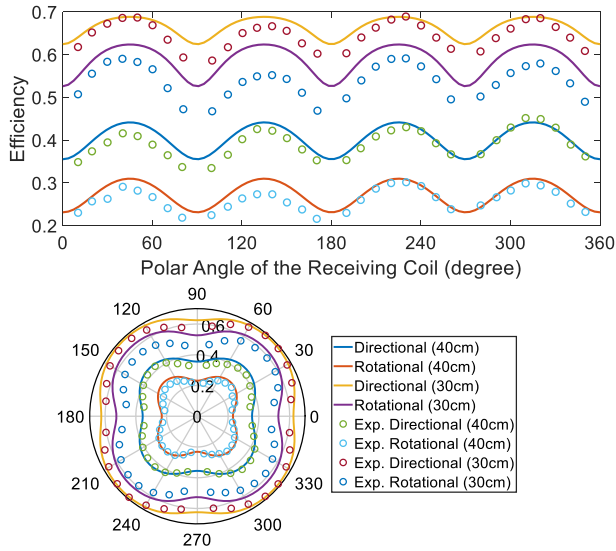
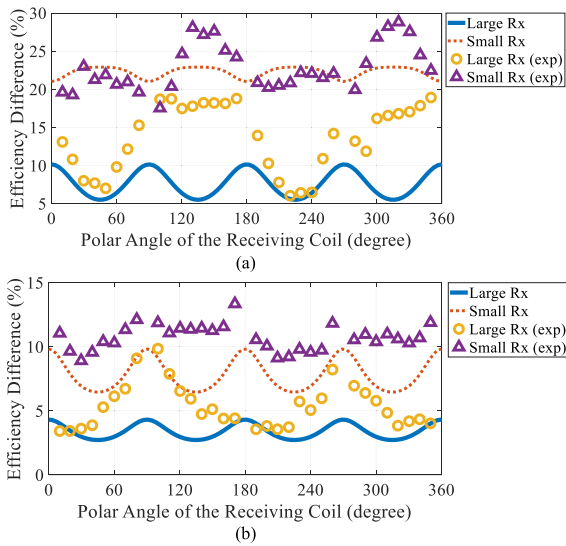Fig. 14. Comparative results of cases 3 and 4 for the small Rx coil.

Fig. 15. Comparative results of efficiency differences between the large Rx coil and the small Rx coil. (a) 40 cm. (b) 30 cm.

TABLE IV
CASES INVESTIGATED FOR MULTIPLE RECEIVERS

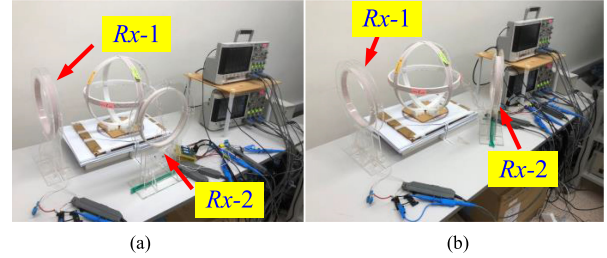| Case	Position	Rx-1	Rx-2	Load-1	Load-2
3	1	small	small	10 Ω	10 Ω
4	1	small	small	50 Ω	10 Ω
5	1	small	small	open	10 Ω
6	1	large	large	10 Ω	10 Ω
7	1	large	large	50 Ω	10 Ω
8	1	large	large	open	10 Ω
9	2	small	small	10 Ω	10 Ω
10	2	small	small	50 Ω	10 Ω
11	2	small	small	open	10 Ω
12	2	large	large	10 Ω	10 Ω
13	2	large	large	50 Ω	10 Ω
14	2	large	large	open	10 Ω

(a)   (b)

Fig. 16. Experimental setup of the 2-D transmitter structure with two receiver loads at the position-1 and position-2. (a) Position-1. (b) Position-2.

TABLE V
OVERALL EFFICIENCY FOR MULTIPLE RECEIVERS

Case	Method	Simulation	Experiment
3	Rotational	62.55%	59.72%
	Directional	66.97%	64.16%
4	Rotational	60.34%	57.93%
	Directional	68.93%	67.04%
5	Rotational	58.78%	55.11%
	Directional	69.06%	68.22%
6	Rotational	76.01%	73.97%
	Directional	78.81%	75.95%
7	Rotational	70.14%	68.4%
	Directional	73.31%	71.21%
8	Rotational	66.68%	62.56%
	Directional	70.83%	69.09%
9	Rotational	62.01%	57.77%
	Directional	66.98%	61.07%
10	Rotational	62.27%	59.22%
	Directional	69.16%	64.17%
11	Rotational	61.17%	55.34%
	Directional	70.32%	65.11%
12	Rotational	78.11%	75.99%
	Directional	80.24%	78.28%
13	Rotational	76.61%	74.57%
	Directional	79.4%	78.21%
14	Rotational	73.71%	72.19%
	Directional	79.39%	79.36%
	Rotational Average (RAv)	**67.37%**	**64.40%**
	Directional Average (DAv)	**72.78%**	**70.16%**
	Efficiency Improvement of the Direactional Method (DAv – RAv)	**5.41%**	**5.76%**

For the directional method, the currents supplied to the transmitter coils are in-phase and the current vector is rotated in discrete angular steps. The ratio of each load power and the total input power over one cycle can be measured and plotted (plots for the cases 3, 4, and 5 are presented in Fig. 17). Based on power efficiency of each load, the overall efficiencies of the
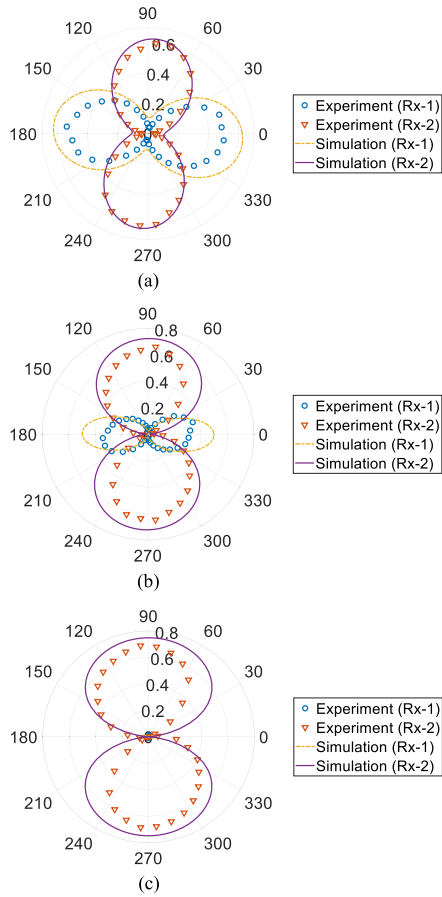
Fig. 17. Power polar plot of the directional WPT for the cases 3, 4, and 5. (a) Case 3. (b) Case 4. (c) Case 5.
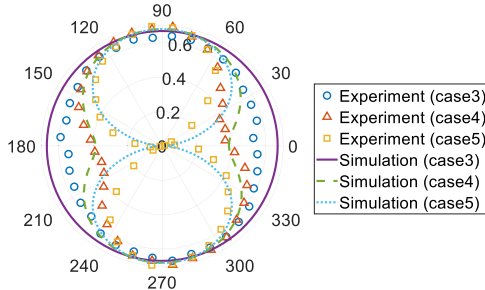

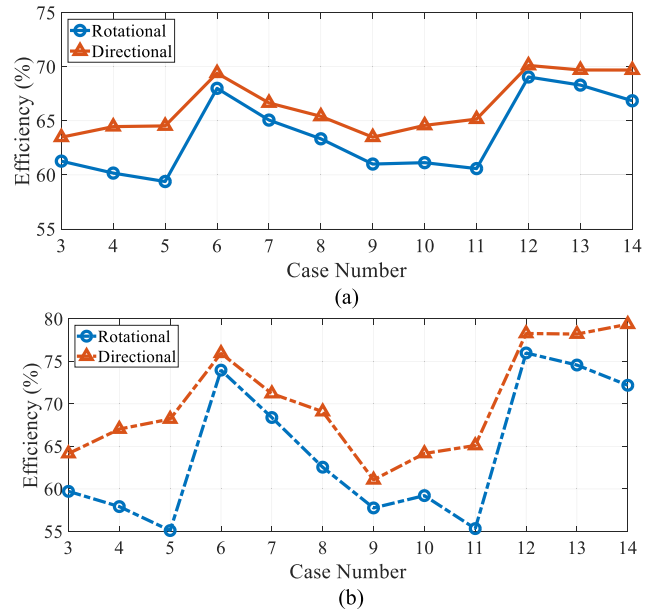Fig. 18. Overall efficiency of the directional WPT for the cases 3, 4, and 5.

Fig. 19. Comparative results of efficiency between the two methods for multiple receivers. (a) Simulation. (b) Experiment.

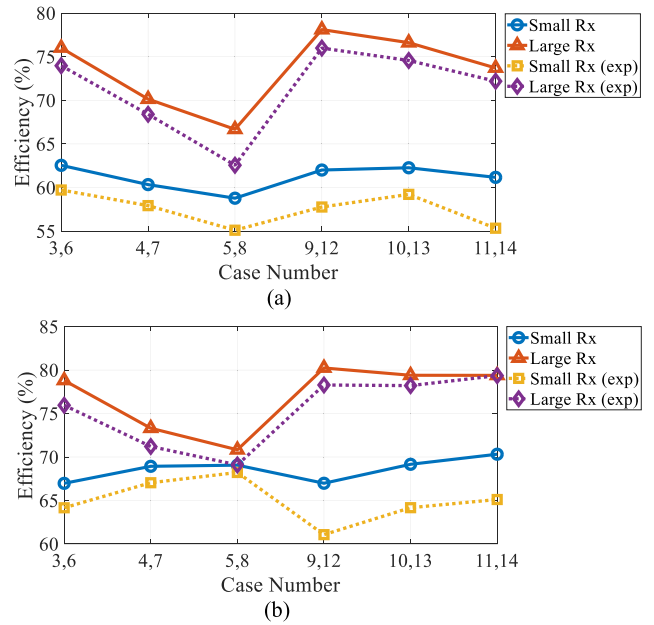
Fig. 20. Comparative results of efficiency between the small Rx coils and the large Rx coils. (a) Rotational. (b) Directional.

directional method can be further plotted (plots for the cases 3, 4, and 5 are presented in Fig. 18). The directional method can search out and control the 2-D WPT system operating at the maximum efficiencies, which are listed in Table V.

The overall efficiencies of all the 12 cases in Table V are depicted in Fig. 19. In both simulation and experiment results, the directional method exhibits higher efficiency than the rotational method for all the cases with different Rx coil positions, Rx coil sizes and load impedances, which validates the analysis and the derived equations in (11). Besides, the efficiencies between the small Rx coils and the large Rx coils are presented in Fig. 20. The results show that the large Rx coils can harvest more energy than

the small Rx coils for both rotational and directional methods when the load conditions are the same. The efficiency differences of the two methods between the large Rx coil and small Rx coil are plotted in Fig. 21. Apparently, the efficiency differences between the two methods are more significant for small Rx coils, which validate the analysis in Fig. 6. The averaged efficiencies of the rotational and directional methods are also calculated and shown in Table V. It is noted that the averaged efficiency of the directional method is 5% higher than that of the rotational counterpart. This result confirms the advantage of the directional WPT approach.
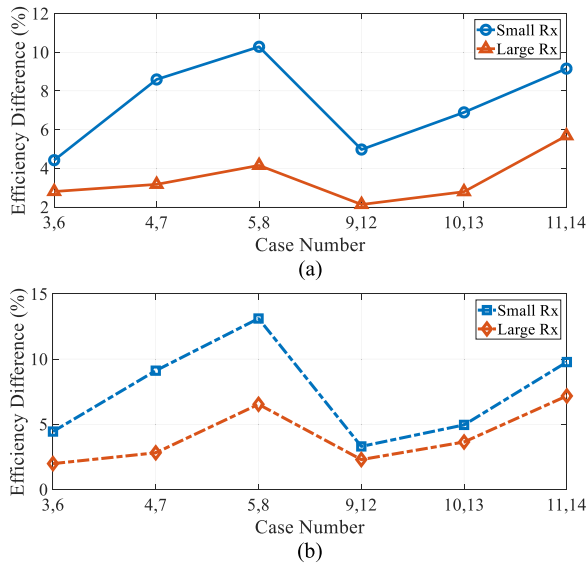
Fig. 21. Comparative results of efficiency difference between the large Rx coils and the small Rx coils. (a) Simulation. (b) Experiment.

IV. CONCLUSION

This article presented a comparative study on the rotational and directional WPT methods for 2-D WPT systems. The directional WPT method presumed the knowledge of load position identification via scanning the power delivered in discrete steps over a cycle so that the transmitter coil currents were controlled to point the resultant magnetic field vector directly toward the loads. The rotational method simplified controls the two transmitter coil currents to rotate the magnetic field vector at high resonant frequency regardless of the locations of the loads. For the first time, a mathematical proof has been developed to show that the directional WPT approach was more efficient than the rotational WPT approach, particularly when the receiver coil sizes become smaller (a situation in which the directional WPT approach was more effective). These findings have been confirmed with both theoretical analysis and practical measurements. The results obtained in the experimental setup confirmed that the energy efficiency of the directional method was at least 5% higher than that of the rotational method. Efficiency improvement of the directional WPT method increased with the dimension differences between the transmitter and receiver coils. The results in this study lead to the following important conclusion. Omnidirectional WPT should preferably adopted the strategy of using the rotational WPT method to scan the power absorption at different angles in order to located the load positions and then used the directional WPT method to focused the wireless power toward the loads for improved performance.

REFERENCES

[1] Wireless power consortium, Oct. 2018. [Online]. Available: https://www.wirelesspowerconsortium.com
[2] S. Y. R. Hui, "Magnetic resonance for wireless power transfer [A look back]," *IEEE Power Electron. Mag.*, vol. 3, no. 1, pp. 14–31, Mar. 2016.
[3] G. A. Covic and J. T. Boys, "Inductive power transfer," *Proc. IEEE*, vol. 101, no. 6, pp. 1276–1289, Jun. 2013.
[4] J. S. Ho, S. Kim, and A. S. Y. Poon, "Midfield wireless powering for implantable systems," *Proc. IEEE*, vol. 101, no. 6, pp. 1369–1378, Jun. 2013.
[5] C. Mi, G. Buja, S. Choi, and C. Rim, "Modern advances in wireless power transfersystems for roadway powered electric vehicles," *IEEE Trans. Ind. Electron.*, vol. 63, no. 10, pp. 6533–6545, Oct. 2016.
[6] S. Hui, "Planar wireless charging technology for portable electronic produts and Qi," *Proc. IEEE*, vol. 101, no. 6, pp. 1290–1301, Jun. 2013.
[7] K. O'Brien, "Inductively coupled radio frequency power transmission system for wireless systems and devices," Ph.D thesis, Technische Universitat Dresden, Dresden, Germany, May 2006.
[8] D. Wang, Y. Zhu, Z. Zhu, T. T. Mo, and Q. Huang, "Enabling multi-angle wireless power transmission via magnetic resonant coupling," in *Proc. Int. Conf. Comput. Convergence Technol.*, 2012, pp. 1395–1400.
[9] O. Jonah, S. V. Georgakopoulos, and M. M. Tentzeris, "Orientation insensitive power transfer by magnetic resonance for mobile devices," in *Proc. IEEE Wireless Power Transfer*, May 2013, pp. 5–8.
[10] W. M. Ng, C. Zhang, D. Lin, and S. Y. Ron Hui, "Two- and Three-Dimensional omnidirectional wireless power transfer," *IEEE Trans. Power Electron.*, vol. 29, no. 9, pp. 4470–4474, Sep. 2014.
[11] W. M. Ng, C. Zhang, D. Lin, and S. Y. R. Hui, "Omni-directional wireless power transfer systems," U.S. Patent 13 975 40, Aug. 2013.
[12] C. Zhang, L. Deyan, and S. Y. R. Hui, "Basic control principles of omnidirectional wireless power transfer," *IEEE Trans. Power Electron.*, vol. 31, no. 7, pp. 5215–5227, Jul. 2016.
[13] D. Lin, C. Zhang, and S. Y. R. Hui, "Mathematical analysis of omnidirectional wireless power transfer—Part-I: Two-dimensional systems," *IEEE Trans. Power Electron.*, vol. 32, no. 1, pp. 625–633, Jan. 2017.
[14] D. Lin, C. Zhang, and S. Y. R. Hui, "Mathematic analysis of omnidirectional wireless power transfer: Part-II three-dimensional systems," *IEEE Trans. Power Electron.*, vol. 32, no. 1, pp. 613–624, Jan. 2017.
[15] J. Feng, Q. Li, and F. C. Lee, "Omnidirectional wireless power transfer for portable devices," in *Proc. IEEE Appl. Power Electron. Conf. Expo.*, 2017, pp. 1675–1681.
[16] J. Feng, M. Fu, Q. Li, and F. C. Lee, "Resonant converter with coupling and load independent resonance for omnidirectional wireless power transfer application," in *Proc. IEEE Energy Convers. Congr. Expo.*, 2017, pp. 2596–2601.
[17] B. H. Choi, E. S. Lee, Y. H. Sohn, G. C. Jang, and C. T. Rim, "Six degrees of freedom mobile inductive power transfer by crossed dipole tx and rx coils," *IEEE Trans. Power Electron.*, vol. 31, no. 4, pp. 3252–3272, Apr. 2016.
[18] Z. Dai, Z. Fang, H. Huang, Y. He, and J. Wang, "Selective omnidirectional magnetic resonant coupling wireless power transfer with multiple-receiver system," *IEEE Access*, vol. pp. 19287–19294, 2018.
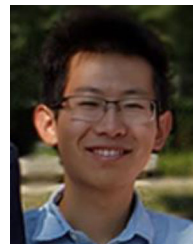
Hanwei Wang received the B.Sc. degree in physics from the Department of Physics, Tsinghua University, Beijing, China, in 2019. He is currently working toward the Ph.D. degree in electrical engineering with the Department of Electrical and Computer Engineering, University of Illinois at Urbana-Champaign, Champaign, IL, USA.

He is interested in developing artificial electromagnetic materials' applications in biomedical imaging and bio-sensors. His research interests include metamaterials, optical force microscopy, magnetic resonance imaging and WPT.
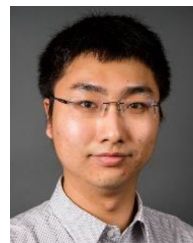
Cheng Zhang (Member, IEEE) was born in China, in 1990. He received the B.Eng. degree (first class Hons.) in electronic and communication engineering from the City University of Hong Kong, Hong Kong, in 2012 and the Ph.D. degree in electronic and electrical engineering from The University of Hong Kong, in 2016.

From 2016 to 2017, he was a Senior Research Assistant with the Department of Electrical and Electronic Engineering, The University of Hong Kong. He was a Postdoctoral Research Associate with the Research Laboratory of Electronics, Massachusetts Institute of Technology, Cambridge, MA, USA from 2017 to 2018. He is currently working with the University of Manchester as a Lecturer in power electronics. His research interests include high-frequency ac–dc power conversions and designs and optimizations for WPT applications.

Yun Yang (Member, IEEE) received the B.Sc. degree from Wuhan University, Wuhan, China, in 2012 and the Ph.D. degree from The University of Hong Kong, Hong Kong, in 2017, both in electrical engineering.

He then became a Postdoctoral Fellow in the same research group. He is currently a Research Assistant Professor with the Department of Electrical Engineering, the Hong Kong Polytechnic University and an Honorary Research Assistant Professor with the Department of Electrical and Electronic Engineering, the University of Hong Kong. He has authored or coauthored more than 40 technical papers, including ten leading journals published as the first author. He also has two book chapters and two U.S. patent applications. His research interests include WPT, microgrid, power electronics and control.

Hui Wen Rebecca Liang (Student Member, IEEE) received the B.S. and M.S. degrees in electrical and electronic engineering from National Cheng Kung University, Tainan, Taiwan, in 2013 and 2015, respectively. She is currently working toward the Ph.D. degree in electrical engineering with the University of Hong Kong, Hong Kong.

In 2015–2017, she worked as an Analog Circuit Engineer with Chroma ATE (Advanced Technology Research Center). Her research interests include power electronics, WPT, dc–dc power converter, and renewable energy conversion.
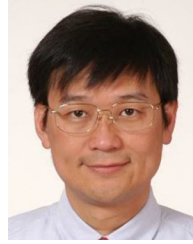
Shu Yuen Ron Hui (Fellow, IEEE) received the B.Sc. (Hons.) degree in electrical and electronic engineering from the University of Birmingham, Birmingham, U.K., in 1984 and the D.I.C. and Ph.D. degrees in electrical engineering from the Imperial College London, London, in 1987.

Previously, he held academic positions with the University of Nottingham and University of Sydney. In 2011–2021, he was the Philip Wong Wilson Wong Chair Professor with the University of Hong Kong. He currently holds the MediaTek Professorship with Nanyang Technological University, Singapore and Chair Professorship of Power Electronics with Imperial College London.

He has authored more than 450 research papers including 300 refereed journal publications. More than 60 of his patents have been adopted by industry worldwide. His research interests include power electronics, wireless power, sustainable lighting, and smart grid.

Dr. Hui inventions on wireless charging platform technology underpin key dimensions of Qi, the world's first wireless power standard, with freedom of positioning and localized charging features for wireless charging of consumer electronics. He also developed the Photo-Electro-Thermal Theory for LED Systems. He was the recipient of the IEEE Rudolf Chope Research and Development Award and the IET Achievement Medal (The Crompton Medal) in 2010 and IEEE William E. Newell Power Electronics Award in 2015. He is a Fellow of the Australian Academy of Technology and Engineering, U.S. National Academy of Inventors and Royal Academy of Engineering, U.K.